Machinery, Materials Science and Engineering Application
Rachid Masrour et al. (Eds.)

© 2026 The Authors.
This article is published online with Open Access by IOS Press and distributed under the terms of the Creative Commons Attribution Non-Commercial License 4.0 (CC BY-NC 4.0).
doi:10.3233/ATDE261161

Mitigation of Forced Van Der Pol Oscillator Vibrations: Nonlinear Energy Sink vs Tuned Mass Damper

Volodymyr PUZYROV [a,b], Nataliya LOSYEVA [a,b], Nina SAVCHENKO [c,1], Javier DIEZ-PALOMAR [a] and Oksana YAROVA [d]
[a] *Universidad de Barcelona, Spain*
[b] *Nizhyn Mykola Gogol State University, Ukraine*
[c] *National Aerospace University, Ukraine*
[d] *State Tax University, Ukraine*

Abstract. Developing effective vibration control strategies is crucial to reducing system vibration and enhancing stability and reliability. In this regard, the study of relatively simple systems that nevertheless demonstrate rich dynamics plays a major role in engineering. One such system is the van der Pol (VDP) oscillator, which can exhibit rich dynamic behavior and effectively describes the nonlinear behavior in various practical engineering systems. In the present work, we study the problem of suppressing the vibrations of a forced self-excited VDP oscillator by means of passive control. Two options are considered: the use of a traditional tuned mass damper (TMD) and a nonlinear energy sink (NES). A semi-analytic tuning approach is suggested to optimize the parameters of both controllers. The results demonstrate that while the TMD is highly effective under specific resonance conditions, the NES offers a broader frequency bandwidth for robust vibration mitigation, providing valuable insights for advanced structural engineering applications and design.

Keywords. Vibration suppression, van der Pol oscillator, frequency-amplitude relation, tuned mass damper, nonlinear energy sink, tuning approach

1. Introduction

Undesirable vibrations are encountered across a broad range of human activities and engineering applications. They arise both from natural causes (seismic activity, wind flows caused by uneven atmospheric heating, ocean currents, increased solar activity, etc.) and from the operation of numerous technical machines and mechanisms. Effective suppression and mitigation of these vibrations are essential for ensuring the reliable and long-term performance of many critical systems that underpin modern society.

For over a century, researchers have proposed numerous vibration control techniques, ranging from passive to active and semi-active methods. Although active and semi-active control offer better performance than passive solutions, they are considerably more expensive, as they require external power sources along with sensors, controllers, and actuators for real-time system adaptation. Passive control relies on pre-

[1] Nina SAVCHENKO, Corresponding author, National Aerospace University, Ukraine; E-mail: n.savchenko@khai.edu.

designed physical characteristics of vibration dampers, operates without external energy input or real-time adaptation, and has been the subject of extensive research.

Nonlinear Energy Sinks (NES) [1] and Tuned Mass Dampers (TMD) [2], also known as vibration absorbers, are among the most widely adopted passive vibration control techniques. The TMD concept was first introduced by Herman Frahm in the early 1900s and was initially applied to reduce vibrations and rolling motion in ship hulls. The theoretical foundation of TMDs was later developed by Ormondroyd and Den Hartog in 1928, with significant contributions by Den Hartog in 1940. Today, TMDs are extensively used in tall buildings, bridges, vehicles, and heavy industrial machinery, where they effectively reduce operational vibrations and enhance overall system performance and efficiency. In recent decades, NES have emerged as a powerful alternative in vibration control, particularly as requirements for equipment reliability and structural safety have become more stringent [3-5]. Compared to conventional TMDs, NES devices often offer advantages such as lighter weight, broader effective frequency range, and greater robustness. Nevertheless, selecting the most suitable device depends on multiple application-specific factors, and the optimal choice is not always obvious.

The van der Pol oscillator (VDP), a well-known self-excited system, is one of the standard models utilized in the study of vibration reduction and limit cycle behavior. The VDP oscillator under forced excitation exhibits rich dynamic behavior due to the complexity of its structure. Based on the relationship between the system's natural frequency ω_0 and the forcing frequency ω, the system displays complex dynamics including synchronization, quasiperiodic motion, and chaos. For many decades, the study of the dynamics of systems akin to the van der Pol oscillator has been a focus of research. This interest has not waned in recent years, both in theoretical [6-8] and practical fields [9-11].

This work aims to test the effectiveness of the previously proposed approach to tuning passive dampers (both linear and nonlinear) [12-14] in suppressing forced self-excited vibrations of the van der Pol oscillator using TMD and NES devices. Results obtained are compared with the paper [15].

2. Formulation of the Problem and Preliminary Transformations

Let us consider a mechanical system schematically presented in figure 1. The system comprises a single-DOF self-excited oscillator of VDP type coupled with a vibration absorber.

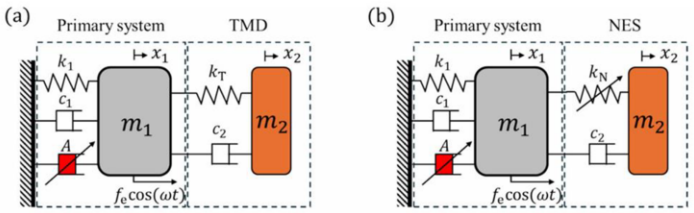

Figure 1. A schematic of a forced self-excited system coupled with (a) TMD and (b) NES (adopted from [15]).

According to [15], we shall discuss two setups: linear TMD and NES. The motion equations of coupled system are

$$m_1\ddot{x}_1 + c_1\dot{x}_1 + c_2(\dot{x}_1 - \dot{x}_2) + k_1x_1 - A_0\dot{x}_1(1 - A_1x_1^2) +$$

$$k_T(x_1 - x_2) + k_N (x_1 - x_2)^3 = f_e \cos(\omega t),$$
$$m_2\ddot{x}_2 + c_2 (\dot{x}_2 - \dot{x}_1) - k_T(x_1 - x_2) - k_N (x_1 - x_2)^3 = 0. \quad (1)$$

Depending on whether we are considering the case of TMD attached or NES, the coefficient k_N (or k_T) is equal to zero. By adding the second equation of (1) to the first one and introducing the new variable $\tilde{x}_2 = x_2 - x_1$, the motion equations may be expressed in a more compact form

$$(m_1 + m_2)\ddot{x}_1 + m_2\ddot{x}_2 + c_1\dot{x}_1 + k_1x_1 - A_0\dot{x}_1(1 - A_1x_1^2) = f_e \cos(\omega t),$$
$$m_2\ddot{x}_1 + m_2\ddot{\tilde{x}}_2 + c_2\dot{\tilde{x}}_2 + k_T\tilde{x}_2 + k_N\tilde{x}_2^3 = 0. \quad (2)$$

Introducing the dimensionless variables, parameters, and time by formulas

$$X_1 = \frac{x_1k_1}{f_e},\ X_2 = \frac{\tilde{x}_2k_1}{f_e},\ \mu = \frac{m_2}{m_1},\ \omega_1 = \sqrt{\frac{k_1}{m_1}}, \kappa_T = \frac{k_T}{k_1},\ \zeta_j = \frac{c_j}{m_1\omega_1}\ (j = 1,2),$$
$$\alpha = \frac{A_0}{m_1\omega_1}, \qquad \beta = A_1\frac{k_1^2}{f_{e,}^2}, \qquad \kappa_N = \frac{k_Nk_1}{f_e^2}, \qquad \Omega = \frac{\omega}{\omega_1}, \tau = \omega t \quad (3)$$

we have

$$\boldsymbol{MX''} + \boldsymbol{DX'} + \boldsymbol{KX} = \boldsymbol{\Phi}(\tau, \boldsymbol{X}, \boldsymbol{X'}). \quad (4)$$

Here

$$\boldsymbol{M} = \Omega^2\begin{pmatrix}1+\mu & \mu\\ \mu & \mu\end{pmatrix}, \boldsymbol{X} = \begin{pmatrix}X_1\\ X_2\end{pmatrix}, \boldsymbol{D} = \Omega\begin{pmatrix}\zeta_1 - \alpha & 0\\ 0 & \zeta_2\end{pmatrix}, \boldsymbol{K} = \begin{pmatrix}1 & 0\\ 0 & \kappa_T\end{pmatrix},$$
$$\boldsymbol{\Phi}(\tau, \boldsymbol{X}, \boldsymbol{X'}) = \begin{pmatrix}-\alpha\beta\Omega X_1'X_1^2 + \cos\tau\\ -\tilde{\kappa}_N X_2^3\end{pmatrix}$$

By introducing a substitution

$$\boldsymbol{X} = \boldsymbol{u}\cos\tau + \boldsymbol{v}\sin\tau, \qquad \boldsymbol{X'} = -\boldsymbol{u}\sin\tau + \boldsymbol{v}\cos\tau,$$

followed by averaging over time τ, we arrive at a system in new variables

$$\boldsymbol{M}\,\boldsymbol{u'} + \frac{1}{2}\,[\boldsymbol{Du} + (\boldsymbol{M} - \boldsymbol{K})\boldsymbol{v}] = \frac{1}{8}\begin{pmatrix}-\alpha\beta\Omega u_1(u_1^2 + v_1^2)\\ 3\tilde{\kappa}_N v_2(u_2^2 + v_2^2)\end{pmatrix},$$
$$\boldsymbol{M}\,\boldsymbol{v'} + \frac{1}{2}[(\boldsymbol{K} - \boldsymbol{M})\boldsymbol{u} + \boldsymbol{D}\,\boldsymbol{v}] = \frac{1}{8}\begin{pmatrix}-\alpha\beta\Omega v_1(u_1^2 + v_1^2) + 4\\ -3\tilde{\kappa}_N u_2(u_2^2 + v_2^2)\end{pmatrix}, \quad (5)$$

The stationary points $(\boldsymbol{u}, \boldsymbol{v})$ of system (5) are determined by following system of nonlinear algebraic equations

$$\boldsymbol{Du} + (\boldsymbol{M} - \boldsymbol{K})\boldsymbol{v} = \frac{1}{4}\begin{pmatrix}-\alpha\beta\Omega u_1(u_1^2 + v_1^2)\\ 3\tilde{\kappa}_N v_2(u_2^2 + v_2^2)\end{pmatrix},$$
$$\boldsymbol{Dv} - (\boldsymbol{M} - \boldsymbol{K})\boldsymbol{u} = \tfrac{1}{4}\begin{pmatrix}-\alpha\beta\Omega v_1(u_1^2 + v_1^2) + 4\\ -3\tilde{\kappa}_N u_2(u_2^2 + v_2^2)\end{pmatrix}, \quad (6)$$

which can be rewritten in complex variables $\boldsymbol{z} = \boldsymbol{u} + i\boldsymbol{v}$ and reads

$$(\Omega\zeta_1 - \Omega\alpha + ib_{11})\,z_1 + ib_{12}z_2 + \gamma\,\Omega\,z_1^2\bar{z}_1 - 1 = 0,$$
$$ib_{12}z_1 + (\Omega\zeta_2 + ib_{22})\,z_2 + i\kappa_N z_2^2\bar{z}_2 = 0, \gamma = \tfrac{1}{4}\alpha\beta, \kappa_N = \tfrac{3}{4}\tilde{\kappa}_N. \quad (7)$$

3. Tuning Methodology for Passive Vibration Absorbers

3.1. Tuning Methodology in TMD Case

Now the NES part is absent; thus $\kappa_N = 0$. This simplifies analysis, since we have a linear relationship between z_1 and z_2. Expressing z_2 from the second equation of (7) and taking the complex conjugate of the first one, we can write the frequency-amplitude relation (FAR) in the following form

$P(\rho_1, \Omega) = \rho_1\,\mu^2\,\Omega^8 + A\,\Omega^6 + B\,\Omega^4 + C\,\Omega^2 + \kappa_N^2(\rho_1 - 1) = 0, \quad \rho_1 = z_1\bar{z}_1$ (8)
where

$A = \rho_1^3\,(\gamma\,\mu)^2 + 2\rho_1^2\,a_1\,\mu^2\,(\zeta_1 + \zeta_2 - 4\gamma) + \rho_1\,[\mu^2\,(\zeta_1 + \zeta_2 + 4\gamma)^2 + \zeta_2^2(1 - \mu^2) + 2\zeta_2\mu - 2\kappa_N\mu(1 + \mu) - 2\mu^2\,], B = \rho_1^3\,(\gamma\,\zeta_2)^2 + 2\rho_1^2\,\gamma\,[7\gamma\kappa_N\mu - 4\zeta_2^2\,\gamma + \zeta_2(\zeta_1 - 2\kappa_N\mu)] + \rho_1\,[\kappa_N^2(\mu^2 + 2\mu + 1) + 2\kappa_N\mu(2 - \zeta_1^2 - 16\gamma^2) - 2\zeta_2^2(1 + \mu + 4\zeta_1\,\gamma - 8\gamma^2) + \mu^2(1 + 2\kappa_N) + \zeta_2^2\,\zeta_1^2\,] - \mu^2, C = \rho_1^3\,(\gamma\,\kappa_N)^2 + 2\rho_1^2\,\gamma\,\kappa_N^2\,(\zeta_1 - 4\gamma) + \rho_1\,[\kappa_N^2\,(\zeta_1 - 4\gamma)^2 + \kappa_N^2(1 - 16\gamma^2) - 2\kappa_N^2(\mu + 1) - 2\kappa_N\mu + \zeta_2^2 + 16\gamma^2\kappa_N^2\,] - \zeta_2^2 + 2\kappa_N\mu.$

Following the idea of peak equalizing as a criterion for the optimal choice of parameters κ_T, ζ_2, the condition for such a choice may be expressed in the following way. Since the expression (8) is a bi-fourth-order polynomial in Ω, peak alignment occurs when this polynomial has repeated roots in Ω^2; that is, it admits representation as $\tilde{P} = \rho_1\mu^2(\Omega^4 - M\Omega^2 + N)^2$. For extremal points $\Omega^{2\,max}_{1,2}$ we can consider the difference of two expressions as identity $P - \tilde{P} = 0$ with respect to Ω^2, having the system of four algebraic equations. Eliminating the unknown value $M = -\frac{A}{2\mu^2\rho_1}$ and considering the condition $\rho_1 = \frac{{\kappa_T}^2}{{\kappa_T}^2 - (\mu N)^2}$, the task reduces to minimizing the quantity N appearing in the system of three algebraic equations, along with the parameters $\mu, \zeta_1, \zeta_2, \alpha, \beta, \kappa_T$. Such technique was described in more detail in the work [16].

Owing to the frictional component in the first equation (2), the closed-form analytical expressions for the optimal pair of values (when the peaks of the frequency-amplitude curve are aligned) cannot be obtained in an exact form [17]. However, considering the mass ratio μ to be a small value, one can obtain asymptotic approximations of these quantities as series on $\sqrt{\mu}$ using various calculation scenarios.

If the mechanical parameters of the primary system (in our case, the SES) are known, the calculation is quite simple from a practical standpoint. We apply the previously described technique [14], which is computationally simple/inexpensive and effective in maximizing the reduction of response peaks. Let us select a certain value as an initial approximation for ρ_1, for example, the peak amplitude of the SES without the absorber, and substitute it into the polynomial P. Since it is assumed that TMD reduces the magnitude of the responses, the equality $P = 0$ is satisfied on some set S_0 of tuning parameters ζ_2, κ_T. By successively decreasing the value of ρ_1, we obtain a sequence of tapering regions $S_1, S_2, \cdots$ that, if the parameters are chosen optimally, will collapse to a point. From a geometric perspective, this appears as shown in figure 2. In order to compare the results, we take the parameter values corresponding to the work [15]:
$\mu = 0.1,\ \zeta_1 = 0.01, \alpha = 0.1, \beta = 1$ (respectively $\eta, \frac{\zeta_1}{2}, \alpha$ in [15]).

The resulting pair of parameters $\kappa_T = 0.077,\ \zeta_2 = 0.037$ is nearly identical to those presented in [15] $\kappa_T = 0.0765,\ \zeta_2 = 0.0336$ (blue and red curves in figure 3a respectively).

3.2. Tuning Methodology in NES Case

Let's turn to system (7). Now $\kappa_N \neq 0$, and this system cannot be solved in closed form for z_1, z_2. However, we are interested in finding relationships between $|z_1|, |z_2|$ and the system parameters. To achieve this, we consider (7) as a linear system (formally considering ρ_1, ρ_2 as coefficients), which leads to

$$z_1 = -\frac{\kappa_N \rho_2 + b_{22} - i\,\zeta_2}{\sigma}, z_2 = \frac{b_{12}}{\sigma},$$

$\sigma = \gamma(\zeta_2 + ib_{22})\,\rho_1 + \kappa_N(i\,\zeta_1 - b_{11})\rho_2 - b_{11}b_{22} + (b_{12})^2 + i(b_{11}\zeta_2 + b_{22}\zeta_1) + \zeta_1\zeta_2.$ Writing down differences $z_i\bar{z}_j - \rho_j = 0, j = 1{,}2$ and performing simplifications, we obtain two polynomials of the following form

$$P_1 = k_{13}\rho_2^3 + k_{12}\rho_2^2 + k_{11}\rho_2 + k_{10},\ P_2 = k_{22}\rho_2^2 + k_{21}\rho_2 + k_{20}, \qquad (9)$$

where

$$k_{13} = \kappa^2(\Omega^2\gamma^2\rho_1^2 + 2\Omega\gamma\zeta_1\rho_1 + b_{11}^2 + \zeta_1^2),$$

$k_{12} = 2\kappa[\Omega^2\gamma^2 b_{22}\rho_1^2 + 2\Omega\gamma b_{22}h_1\rho_1 + b_{11}(b_{11}b_{22} - b_{12}^2) + b_{22}h_1^2],$
$k_{11} = \Omega^2\gamma^2(b_{22}^2 + \zeta_2^2)\rho_1^2 + 2\Omega\gamma(b_{12}^2\zeta_2 + b_{22}^2\zeta_1 + \zeta_1\zeta_2^2)\rho_1 + (b_{11}b_{22} - b_{12}^2)^2 + b_{22}^2\zeta_1^2 + b_{11}^2\zeta_2^2 + 2b_{12}^2\zeta_1\zeta_2 + \zeta_1^2\zeta_2^2, k_{10} = -b_{12}^2, k_{22} = \kappa^2[\Omega^2\gamma^2\rho_1^3 + 2\zeta_1\Omega\gamma\rho_1^2 + (b_{11}^2 + \zeta_1^2)\rho_1 - 1], k_{21} = 2\kappa[\Omega^2\gamma^2 b_{22}\rho_1^3 + 2b_{22}\zeta_1\Omega\gamma\rho_1^2 + (b_{11}(b_{11}b_{22} - b_{12}^2) + b_{22}\zeta_1^2 + b_{22}b_{11}^2)\rho_1 - b_{22}], k_{20} = \Omega^2\gamma^2(b_{22}^2 + \zeta_2^2)\rho_1^3 + 2\Omega\gamma(b_{12}^2\zeta_2 + b_{22}^2\zeta_1 + \zeta_1\zeta_2^2)\rho_1^2 + [(b_{11}b_{22} - b_{12}^2)^2 + b_{11}^2\zeta_2^2 + b_{22}^2\zeta_1^2 + 2b_{12}^2\zeta_1\zeta_2 + \zeta_1^2\zeta_2^2]\rho_1 - b_{22}^2 - \zeta_2^2, b_{11} = k_1 - (1+\mu)\Omega^2, b_{12} = -\mu\Omega^2, b_{22} = k_a - \mu\Omega^2.$

Equalities (9) relate the squares of the oscillation amplitudes in terms of the variables $\boldsymbol{u}, \boldsymbol{v}$ (or equally, in dimensionless displacements X_1, X_2) as functions of the frequency ratio Ω and the system parameters. Owing to their multiparametric nature, these relations are of little use for direct analysis. However, provided the VDP oscillator's configuration is known, they are quite suitable for tuning the NES parameters. Calculating the expression for resultant of polynomials P_1, P_2 in ρ_2, we arrive to direct FAR for $|X_1|$. Now we have a ninth-order polynomial in ρ_1. Although the remark of previous sub-section regarding the existence of multiple roots in Ω^2 remains valid, the polynomial P_{res} now also has complex roots, which significantly complicates the analysis. However, the numerical procedure based on the same "hollow-seeking" scheme works without serious complications. After six iterations we find the following pair $\kappa_T = 0.0027,\ \zeta_2 = 0.053$.

The figure 3b shows the FA curve. Unlike choice made in [15] (the red curve in figure 3b), our pair has reduced response values and two distinct peaks. However, as demonstrated by the authors of [15], only one peak is present, indicating that their NES setup is insufficiently optimal.

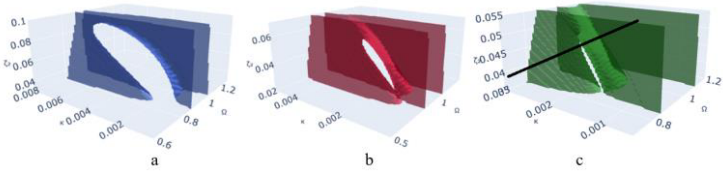

Figure 2. Visualization of the "hollow-seeking" approach for locating the optimal tuning parameters.

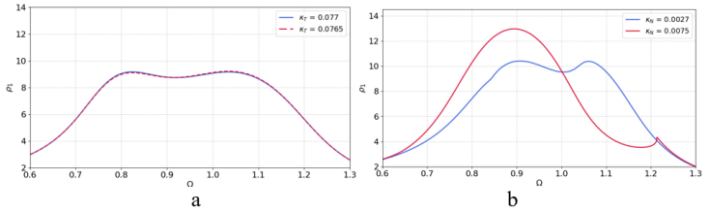

Figure 3. Frequency-amplitude dependence. Comparing the tuning results with [15]: a) TMD attached; b) the case of NES.

Note that although the polynomial utilized in constructing the FA curve is much more cumbersome than P in subsection 3.1, by substituting the value $\kappa_N = 0$ and choosing the other parameters according to the TMD configuration, the resulting curve exactly matches the one shown in figure 3a.

4. Numerical Validation

To verify the results presented in the previous section, we carried out numerical integration both for systems (4) and (5). The trajectories and phase portraits of the considered dynamical system were modeled using the Python programming language and its specialized scientific computing libraries. Numerical integration of the system of differential equations was performed via the solve_ivp function from the SciPy package, employing the explicit 4th/5th-order Runge-Kutta method (Dormand-Prince pair, RK45 algorithm) with an adaptive step-size control. Visualization of the results and graphical rendering of the phase planes were carried out using the Matplotlib library.

Figure 4 illustrates that, over time, both the main system and the absorber (for TMD as well as NES) reach their limit cycles. In the TMD case, the limit cycles shapes of the main system and the absorber are quite similar. For the NES, however, the situation is different: due to the distinct types of nonlinearity (x^3 vs $\dot{x}x^2$), the shape of the NES limit cycle differs noticeably from that of the VDP oscillator. It is also evident that the size of these limit cycles agrees well with results shown in figure 3. Regarding the trajectories in "slow" variables (figure 5), the transient behavior in the NES case tends to be more intricate, as can be observed in the right part of figure 5b.

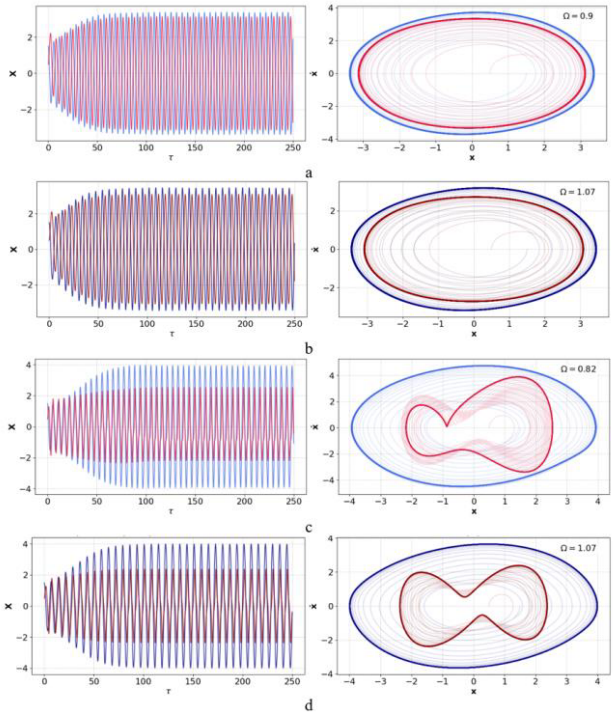

Figure 4. Time histories and phase trajectories corresponding to set of parameters in figure 3.

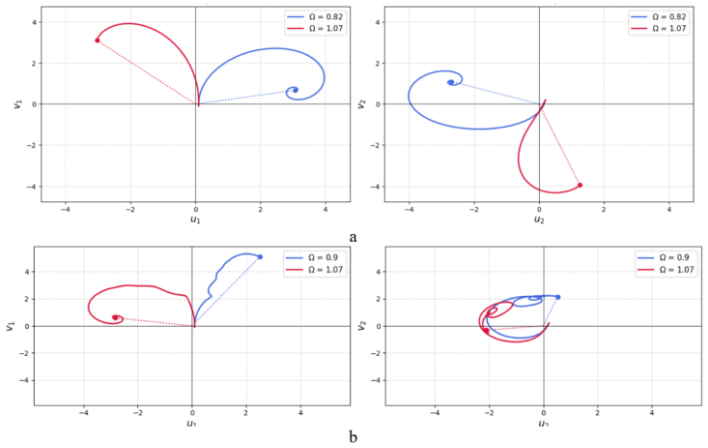

Figure 5 Phase trajectories in "slow" variables u, v attracting to stationary point of system (7): a is related to TMD and b - to NES. The blue color corresponds to X_1 displacement, and the red one to X_2.

The distances from the initial conditions to the attractor are in good agreement with the frequency ratio values at the two peaks of the FA curve.

Stability and bifurcation issues were not considered in the present study. A similar analysis from a technical standpoint can be found in [13]. As illustrated in figures 4 and 5, for the particular configuration of system (1) examined here, the stationary point acts as an attractor, and no bifurcations occur.

5. Conclusion

This study addresses the problem of vibration suppression of self-excited system of van der Pol oscillator using two different types of passive dynamic absorbers: tuned mass damper and nonlinear energy sink. The averaging method is employed to eliminate the explicit presence of time from analysis. The steady state responses are examined, and optimal configuration of absorbers is suggested. For case study presented earlier in paper [15] the optimal configuration of TMD is the same, but for NES it differs and allows to suppress peaks of vibration with more efficiency. These results are compared with the similar ones from literature and validated by numerical simulations. The future work will be related to the analysis of the combined influence of linear and nonlinear components of absorbers on their efficiency.

Author Contributions

Conceptualization, Puzyrov V; Data curation, Puzyrov V and Losyeva N; Formal analysis, Puzyrov V; Methodology, Puzyrov V; Software, Puzyrov V and Savchenko N; Supervision, Puzyrov V and Losyeva N; Validation, Puzyrov V and Diez-Palomar J; Visualization, Puzyrov V and Savchenko N; Writing – original draft, Puzyrov V; Writing – review & editing, Puzyrov V, Losyeva N, Savchenko N and Yarova O. All authors have read and agreed to the published version of the manuscript.

Conflicts of Interest

The authors declare no conflict of interest.

References

[1] Ding H, Chen LQ. Designs, analysis, and applications of nonlinear energy sinks. Nonlinear Dyn. 2020; 100(4): 3061–3107. https://doi.org/10.1007/s11071-020-05724-1

[2] Yang F, Sedaghati R, Esmailzadeh E. Vibration suppression of structures using tuned mass damper technology: A state-of-the-art review. J. Vib. Control. 2022; 28(7–8): 812–836. https://doi.org/10.1177/1077546320984305

[3] Liu J, Lu ZQ, Wang M, Pu HY, Sun Y, Ding JH, Peng Y, Xie SR, Luo J. A tunable electromagnetic nonlinear energy sink. Chaos Solitons Fractals. 2024; 188: 115453. https://doi.org/10.1016/j.chaos.2024.115453

[4] Jin Y, Liu K, Xiong L, Tang L. A non-traditional variant nonlinear energy sink for vibration suppression and energy harvesting. Mech. Syst. Signal Process. 2022; 181: 109479. https://doi.org/10.1016/j.ymssp.2022.109479.

[5] Sun Z, Zhao J, Zhang C, Yuan S, Zheng X, Luo J, Pu H. Investigation of a nonlinear energy sink based on magnetic inerter. Acta Mech. Sin. 2025; 41(10): 524407. https://doi.org/10.1007/s10409-024-24407-x

[6] Afzali F, Kharazmi E, Feeny BF. Resonances of a forced van der Pol equation with parametric damping. Nonlinear Dyn. 2023; 111: 5269–5285. https://doi.org/10.1007/s11071-022-08026-w

[7] Han X, Bi Q. Effects of amplitude modulation on mixed mode oscillations in the forced van der Pol equation. Nonlinear Dyn. 2023; 111(14): 12921–12930.

[8] Wang Y, Li X & Shen Y. Study on mechanical vibration control of limit cycle oscillations in the van der pol oscillator by means of nonlinear energy sink. J. Vib. Eng. Technol. 2024; 12: 811–819. https://doi.org/10.1007/s42417-023-00877-w

[9] Cui W, Zhao L, Ge Y, et al. A generalized van der Pol nonlinear model of vortex-induced vibrations of bridge decks with multistability. Nonlinear Dyn. 2024; 112: 259–272. https://doi.org/10.1007/s11071-023-09047-9

[10] Hajj MR, Mehmood A, Akhtar I. Single-degree-of-freedom model of displacement in vortex-induced vibrations. Nonlinear Dyn. 2021; 103(2): 1305–1320.

[11] Wang Y, Li X, Shen Y. Vibration reduction mechanism of Van der Pol oscillator under low-frequency f orced excitation by means of nonlinear energy sink. Int. J. Non-Linear Mech. 2023; 152: 104389. https: //doi.org/10.1016/j.ijnonlinmec.2023.104389.

[12] Puzyrov V, Awrejcewicz J. Asymptotical stability of the motion of mechanical systems with partial ene rgy dissipation. Nonlinear Dyn. 2018; 91: 329–341. https://doi.org/10.1007/s11071-017-3873-x.

[13] Puzyrov V, Losyeva N, Savchenko N. Nonlinear vibration isolator with softening spring and nonlinear damping. Adv. Transdiscip. Eng. 2024; 58: 503–511. https://doi.org/10.3233/ATDE240666

[14] Puzyrov V, Losyeva N, Savchenko N. Vibration control using a quasi-zero stiffness inerter: The tuning approach. Adv. Transdiscip. Eng. 2025; 79: 373 - 378. https://doi.org/10.3233/ATDE251003

[15] Chao C, Dai W, Shi B, Branson D, Yang J. Suppression of self-excited vibrations using tuned mass dam per or nonlinear energy sink. Nonlinear Dyn. 2025; 113: 32007–32035. https://doi.org/10.1007/s11071-025-11769-x

[16] Puzyrov V, Awrejcewicz J. On the optimum absorber parameters: revising the classical results. J. Theo r. Appl. Mech. 2017; 55(3): 1081–1089. https://doi.org/10.15632/jtam-pl.55.3.1081.

[17] Warburton GB, Ayorinde EO. Optimum absorber parameters for simple systems. Earthquake Eng. Stru ct. Dyn. 1980; 8: 197–217.